JGR Oceans

RESEARCH ARTICLE
10.1029/2022JC019418

Key Points:

- Recent Pacific Summer Water (PSW) warming in the Canada Basin is accompanied by dissolved oxygen decreases in the same water mass
- Decreased oxygen solubility due to warming of source waters can account for dissolved oxygen decreases in the upper PSW
- Lower PSW dissolved oxygen decreases are attributed to both physical (~44%) and biological (~56%) effects of the warming

Supporting Information:

Supporting Information may be found in the online version of this article.

Correspondence to:

A. Arroyo,
ashley.arroyo@yale.edu

Citation:

Arroyo, A., Timmermans, M.-L., Le Bras, I., Williams, W., & Zimmermann, S. (2023). Declining O_2 in the Canada Basin halocline consistent with physical and biogeochemical effects of Pacific summer water warming. *Journal of Geophysical Research: Oceans*, *128*, e2022JC019418. https://doi.org/10.1029/2022JC019418

Received 26 OCT 2022
Accepted 5 MAR 2023

Declining O_2 in the Canada Basin Halocline Consistent With Physical and Biogeochemical Effects of Pacific Summer Water Warming

Ashley Arroyo[1], Mary-Louise Timmermans[1], Isabela Le Bras[2], William Williams[3], and Sarah Zimmermann[3]

[1]Department of Earth and Planetary Sciences, Yale University, New Haven, CT, USA, [2]Department of Physical Oceanography, Woods Hole Oceanographic Institution, Woods Hole, MA, USA, [3]Fisheries and Oceans Canada, Institute of Ocean Sciences, Sidney, BC, Canada

Abstract The Arctic Ocean's Canada Basin (CB) has seen significant changes in ocean properties in the past two decades. A prominent change has been a warming of the Pacific Summer Water (PSW) layer in the central CB. The corresponding change in dissolved oxygen (O_2) is analyzed here to provide additional insight into PSW physics and biology, pathways, and evolution. O_2 observations are analyzed between 2003 and 2021 from the Joint Ocean Ice Study/Beaufort Gyre Observing System (JOIS/BGOS) field program, which samples CB hydrographic and biogeochemical properties. In the central CB, warming of the PSW layer over 2003–2021 has been accompanied by O_2 decreases over this time in the layer. Nutrients and other biogeochemical properties are analyzed to quantify the combined influences of both physical changes and biological changes on the evolution of O_2 concentrations in the CB PSW. In the upper portion of the PSW, O_2 decreases can be entirely accounted for by surface warming (and corresponding decrease in O_2 solubility) of its source waters in the Chukchi Sea region. In the deeper portion of the PSW layer, the observed O_2 changes are larger, and are accounted for by a combination of the decreased solubility effect due to warming, and increased organic matter breakdown in warmer waters. Decreasing O_2 in a warming Arctic Ocean is consonant with O_2 trends in the warming global oceans, and highlights the need for continued observations and analyses.

Plain Language Summary Water properties in the Arctic Ocean's Canada Basin have changed significantly over the past two decades. The most prominent change has been a warming of a water layer sourced from the Pacific Ocean. It is shown here that this warming has been accompanied by a decrease in dissolved oxygen in the same water layer. The warming and oxygen decline are analyzed in context to gain insight into how and why the Arctic Ocean is changing. Ship-based data from annual icebreaker expeditions, which include measurements of temperature, salinity, dissolved oxygen, and nutrients, are analyzed. The analysis suggests that physical and biological processes have different influences in the different parts of the water layer. In recent decades, widespread dissolved oxygen decreases have also been observed in the global oceans because of ocean warming. This study documents similar changes underway in the Arctic Ocean.

1. Introduction

Pacific waters enter the Arctic Ocean via the Bering Strait and flow into the Chukchi Sea (Woodgate et al., 2005) where they are modified at the surface before subducting beneath the polar mixed layer of the Canada Basin (CB, Figure 1a) to ventilate the halocline. The Pacific halocline in the CB plays an important role in regulating climate, as the strong stratification prevents subsurface ocean heat from penetrating into the surface mixed layer, and melting sea ice (Aagaard et al., 1981). Water sourcing from the Pacific Ocean has two variants: warm Pacific Summer Water (PSW), which ventilates the CB halocline during the summer to reside immediately beneath the CB mixed layer and Pacific Winter Water (PWW), which ventilates the CB in winter to reside under the PSW layer (e.g., Coachman & Barnes, 1961; Steele et al., 2004; Timmermans et al., 2014, 2017); see Figure 1b. One of the most prominent recent changes in the CB has been a substantial increase in heat content of the CB PSW layer, which has approximately doubled over 2003–2021 (Timmermans & Toole, 2023; Timmermans et al., 2018). Here we explore the distribution and evolution of dissolved oxygen (O_2) of the PSW as it relates to temperature, salinity, and nutrients to better understand its pathways and governing processes.

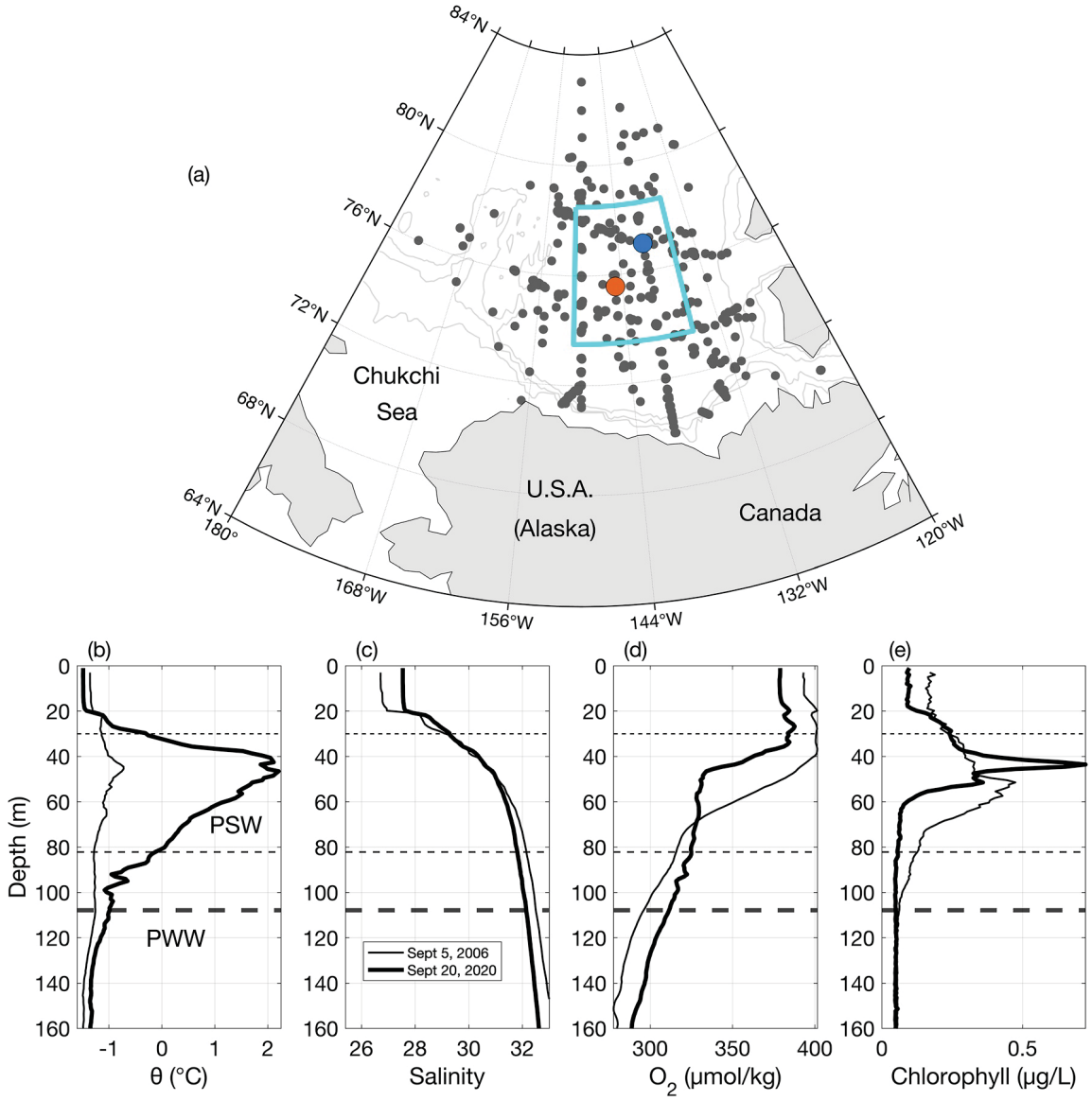

Figure 1. (a) Map of the Canada Basin (CB) region showing hydrographic station locations from annual 2003–2021 Joint Ocean Ice Study/Beaufort Gyre Observing System (JOIS/BGOS) expeditions. The cyan box shows the central CB region. The blue dot shows the location of hydrographic profiles in (b–e) and the orange dot shows the location of the profiles in Figure 6. The 1,000, 300, and 100 m isobaths are shown in light gray. (b) Potential temperature (c) salinity (d) O_2 and (e) Chlorophyll fluorescence versus depth. Black dashed lines indicate 30 m depth, and thin and thick dashed lines indicate the depths of the $S = 32.3$ isohaline for 2006 and 2020 respectively.

O_2 concentrations generally decrease with depth through the Pacific halocline (Figure 1d). O_2 is set at the surface by a combination of physical and biological influences, including temperature (which determines solubility), sea-ice extent (which influences gas exchange and light availability), melt and growth, and primary production (Eveleth et al., 2014; Falkner et al., 2005; Ouyang et al., 2021; Timmermans et al., 2010). O_2 concentrations below the surface in the CB (in the PSW) likely reflect surface conditions when waters were last in contact with the atmosphere in the Chukchi Sea, as well as some modification along pathways and during residence in the CB. At depths where both light levels and nutrient concentrations are sufficiently high to support primary production, a subsurface chlorophyll maximum is often observed (Ardyna et al., 2013; Martin et al., 2012); this depth generally coincides with the depth of the PSW temperature maximum (Figures 1b and 1e). The extent to which the peak in primary productivity, indicated by the subsurface chlorophyll maximum, influences the seasonal cycle of O_2 in the CB's Pacific halocline is not well understood. O_2 in PSW is also modified by remineralization (i.e., consumption of O_2 during the breakdown of organic matter to its inorganic constituents such that

nutrient concentrations are increased); this occurs below the subsurface chlorophyll maximum in PSW, resulting in decreasing O_2 concentrations (and increasing nutrient concentrations) with depth through the PSW layer as sinking organic matter breaks down.

In this study, we analyze O_2 observations (in context with other oceanographic properties) in the CB during annual ice-breaker expeditions under the Joint Ocean Ice Study/Beaufort Gyre Observing System (JOIS/BGOS) field program over 2003–2021. We explore the evolution of O_2 in the PSW layer in context with the physical changes that have been documented previously. In the next section, the data are described, quantities used to express O_2 are explained, and the Pacific sourced layers in the CB are characterized. Section 3 describes the spatial variability of O_2 and temperature in the CB PSW. Section 4 describes how O_2 evolves alongside PSW warming over 2003–2021, and Section 5 investigates the mechanisms driving O_2 changes in PSW over the study duration. The results are summarized and discussed in Section 6.

2. Methods

2.1. Data

Data analyzed are from annual hydrographic surveys (from 2003 to 2021) of the Canadian Coast Guard Ship *Louis S. St-Laurent* in the CB under the JOIS/BGOS program, which provide an extensive record of ocean physical and biogeochemical properties; annual surveys take place sometime between July and October each year at a set of repeat sites (Figure 1 and Figure S1 in Supporting Information S1). The hydrographic profile data were collected via CTD/Rosette casts equipped with at least one SeaBird Electronics 43 (SBE-43) dissolved oxygen sensor. Biological and geochemical parameters including O_2, nutrients, and chlorophyll A (Chl A) were also measured in water samples from the Niskin bottles housed in the Rosette (see McLaughlin et al., 2009). The O_2 data from the SBE-43 sensor(s) were calibrated using the SeaBird Inc. lab calibration and comparisons to water samples from the Niskin bottles, including between-station drift corrections (typically <2.2 μmol kg^{-1}) and a final adjustment to remove a pressure dependent shape in the residuals (typically <6.5 μmol kg^{-1}). Accuracy is based on the standard deviation with O_2 water samples from the bottles; comparison with water samples for each yearly expedition typically gives a standard deviation of 3.5 μmol kg^{-1} for all samples. Two sets of samples of nutrients (nitrate and phosphate) were collected from the Niskin bottles, where one set was analyzed onboard within 12–24 hr of collection, and the other was stored at −20°C in the case that further analysis was needed. The unfiltered nutrients were analyzed using a nutrient Auto-Analyzer (see McLaughlin et al., 2009), following the methods described in Barwell-Clarke and Whitney (1996). We augment the JOIS/BGOS data to explore a broader region, including the Chukchi Sea, with observations from the World Ocean Database 2018 (WOD18, Boyer et al. (2018)). WOD18 data include 2263 CTD profiles and 550 bottle-data profiles, and span 2000 to 2017 (Boyer et al., 2018). O_2 data from bottle samples were stated to have an uncertainty of ∼1 μmol kg^{-1} (Boyer et al., 2018).

2.2. Quantifying O_2 Changes

Other quantities can be analyzed alongside O_2 to aid in understanding the mechanisms driving its variability. O_2 solubility $[O_2]_{sol}$ is the amount of O_2 that surface waters in equilibrium with the atmosphere can absorb, and is a function of ocean temperature, salinity and atmospheric pressure (Garcia & Gordon, 1992). These parameters influence the solubility in different magnitudes, with $[O_2]_{sol}$ being mainly a function of temperature, and less dependent on salinity and pressure. O_2 solubility is useful in identifying changes in O_2 purely due to physical properties. For example, warmer waters have a lower O_2 solubility than cooler waters, which means that warm surface waters in equilibrium with the atmosphere will be characterized by lower O_2 compared to cooler waters.

Apparent Oxygen Utilization (AOU) is defined as the difference between O_2 solubility and in situ O_2,

$$AOU = [O_2]_{sol} - [O_2]. \quad (1)$$

These differences arise from mixing, and the biological effects of photosynthesis and respiration. Positive AOU values are generally attributed to consumption of O_2 by respiration and the breakdown of organic matter (Garcia et al., 2013). Negative AOU values can arise in surface waters where O_2 concentrations can be elevated above saturation by primary production. In the surface Arctic Ocean, negative values may be observed when O_2-rich

waters are expelled during sea-ice growth (see e.g., Timmermans et al., 2010). AOU may be used to analyze changes in ventilation of ocean subsurface layers; for example, poorly ventilated water masses generally have high AOU (due to the respiration without replenishment by photosynthesis or interaction with the atmosphere) compared to an efficiently ventilated water mass (Koeve & Kähler, 2016).

2.3. Characterizing the Pacific Summer Water (PSW)

For the purpose of this study, the PSW is defined to be the layer between a depth of 30 m and the depth of the $S = 32.3$ isohaline (Figures 1b–1e). We analyze only waters deeper than 30 m to minimize seasonal influences shallower than this (see Timmermans & Toole, 2023); the varied timing of the annual expeditions can mean significantly different surface-water properties (see Figure S1 in Supporting Information S1). The deep bound for the layer is chosen to be the isohaline closest to the local temperature minimum at the base of the PSW, and is consistent with the upper bound of the PWW ($\sigma = 26$ kg m^{-3}) used by Zhong et al. (2019). Partial profiles that begin deeper than 30 m or end shallower than the depth of $S = 32.3$ are omitted. For each profile, layer-averaged values of potential temperature $\overline{\theta}$ and dissolved oxygen $\overline{O_2}$ are computed as the depth integrals of these quantities divided by PSW layer thickness. Examination of properties has further indicated that it is useful to partition the PSW into upper and lower portions separated at the depth of the PSW temperature maximum in any profile. In select analyses where indicated, only profiles in the central Canada Basin (CCB) region (73.5–78.5°N and 151°W–135.5°W, cyan box in Figure 1a) are considered to avoid spatial variability toward the boundaries of the basin; we refer to this region as the CCB. For year-to-year comparisons of CCB PSW, temperature and oxygen profiles are linearly interpolated onto a 0.1 salinity grid, spanning $S = 26$ to 35. The mean potential temperature and oxygen values at each salinity grid point are taken to construct mean quantities for each year. Working in salinity coordinates rather than depth space avoids the influence of water-column heaving causing spurious property differences between profiles.

3. Dissolved Oxygen in Canada Basin PSW

The spatial variability of PSW $\overline{O_2}$ and $\overline{\theta}$ in the CB is shown for 3 year groups spanning 2003–2021 (Figure 2). A prominent feature of PSW is the warm Alaskan Coastal Water, ACW (Steele et al., 2004) seen in the southwest CB region (Figures 2a–2c). The $\overline{O_2}$ concentrations associated with the ACW current are anomalously high compared to the rest of the basin in the early years, and low in the later years (Figures 2d–2f). The ACW is subject to strong seasonal variability (e.g., Weingartner et al., 2005), and the timing of the annual expeditions varies slightly from year-to-year (see Figure S1 in Supporting Information S1 for annual cruise timing). These monthly differences in sampling may account for $\overline{O_2}$ and $\overline{\theta}$ differences in temporal comparisons at the boundaries of the CB, especially those of the seasonal ACW.

In general, the northern boundaries of the CB (at latitudes north of about 78°N) have lower $\overline{\theta}$ values relative to its central region and southern boundaries. Similar to the spatial patterns in $\overline{\theta}$, $\overline{O_2}$ values tend to be relatively low in the north. This transition to low $\overline{O_2}$ from south to north relates to the transition from the Pacific halocline to the Eurasian Basin halocline (Timmermans et al., 2010), and is commensurate with a thinner layer in the north compared to the south (Figures 2g–2i). Note that the PSW is thickest in the CCB (Figures 2g–2i); its bottom bounding isohaline is up to 100 m deeper there in comparison to its margins (see Timmermans & Toole, 2023).

Although there is significant spatial variability in the properties over the CB, the central basin region shows a clear temporal evolution toward a warmer and thicker PSW layer (Figure 2); the recent increases in PSW heat content (see Timmermans et al., 2018) are attributed to both the warming and thickening of the layer. Along with the PSW warming and thickening, there is a trend toward reduced dissolved oxygen (Figure 2). To quantify this change while avoiding the influence of spatial variability and boundary regions strongly influenced by seasonal variability, we next consider only the central CB, CCB (bounded by the cyan boxes in Figures 1a and 2a).

4. Evolution of O_2 in the Central Canada Basin

The CCB shows a relatively uniform spatial distribution of $\overline{\theta}$ and $\overline{O_2}$ values, and here we consider only profiles in the CCB to analyze the interannual progression of PSW warming and dissolved oxygen decreases (Figure 3).

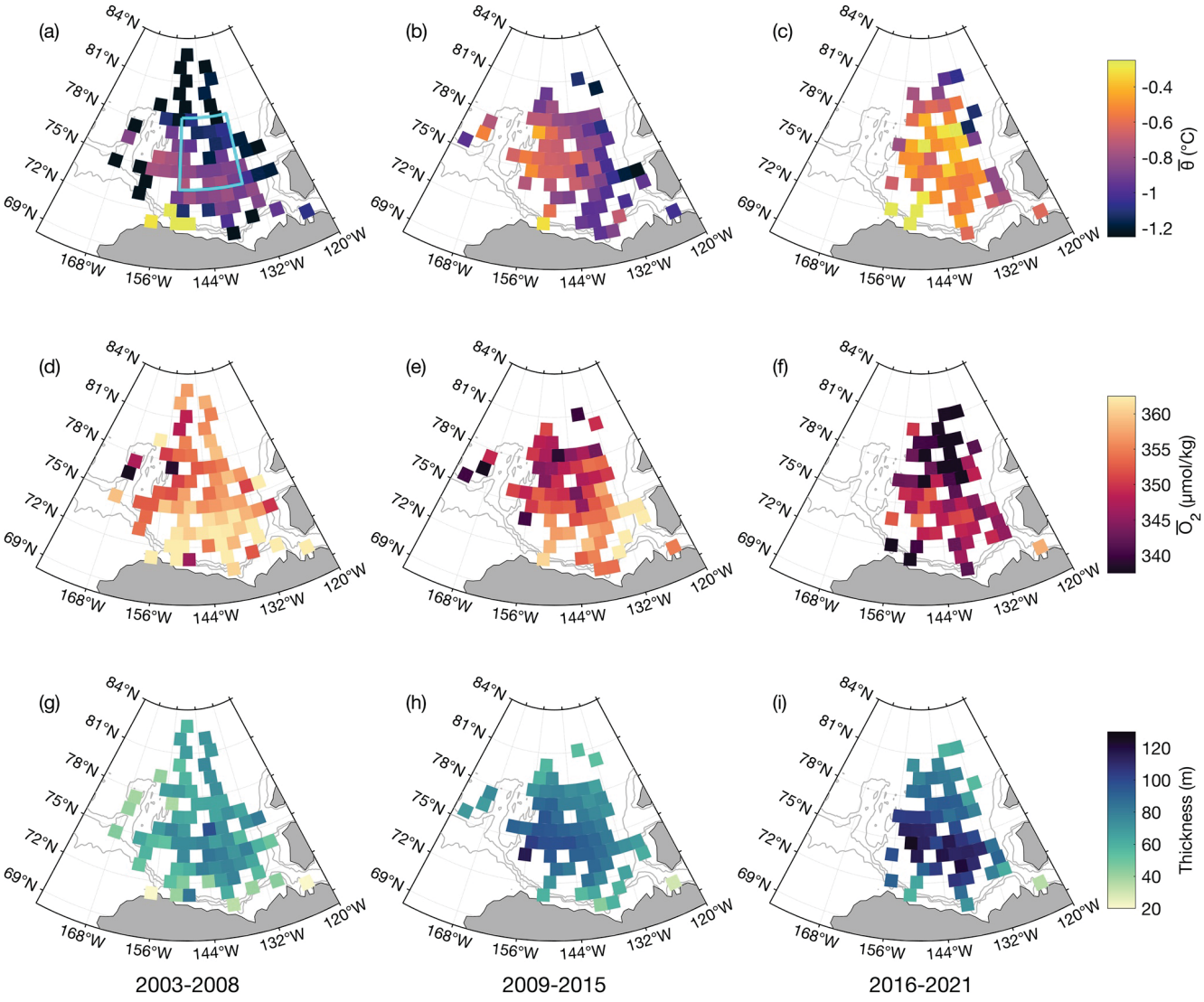

Figure 2. (a–c) Layer-averaged potential temperature ($\overline{\theta}$, °C) (d–f) layer-averaged dissolved oxygen ($\overline{O_2}$, μmol kg^{-1}) and (g–i) Pacific Summer Water layer thickness (m) over 3 year groups (2003–2008, left column; 2009–2015, middle column; 2016–2021, right column). Each square represents the mean value over all profiles within a 100 km × 100 km grid cell. The 1,000, 300, and 100 m isobaths are shown in gray. The cyan box in (a) shows the central Canada Basin region. Refer to Figures S2 and S3 in Supporting Information S1 that show standard deviation of the quantities and number of stations in each grid cell respectively.

Potential temperature and dissolved oxygen profiles (Figure 3) indicate that the most significant warming and strongest O_2 decreases are in the PSW layer (bounded by the vertical dashed lines in Figure 3).

To provide context for the trends observed in PSW, we briefly examine the evolution of θ and O_2 in other layers of the water column. In PWW, which is defined as the water between the depth of the $S = 32.3$ isohaline (the lower bound of PSW) and the depth of the $S = 33.6$ isohaline (consistent with the lower bound for PWW of $\sigma = 27$ kg m^{-3} used by Zhong et al. (2019)), there is negligible change in each of the corresponding layer-averaged properties. In the Atlantic Water layer, which resides directly beneath the PWW layer, θ and O_2 show increasing/decreasing trends respectively (although with much smaller property changes than for the PSW). Since the PSW layer shows significantly more change than any other layer in the upper water column, we restrict our analysis here to this layer.

The changes in θ and O_2 over 2003–2021 are observed through the entire PSW layer, but are not necessarily uniform with depth. The depth range of maximum O_2 change sits deeper ($S \approx 31.4$) than the depth range of maximum θ ($S \approx 30.4$, Figures 3a and 4), suggesting that different processes may be contributing to O_2 change

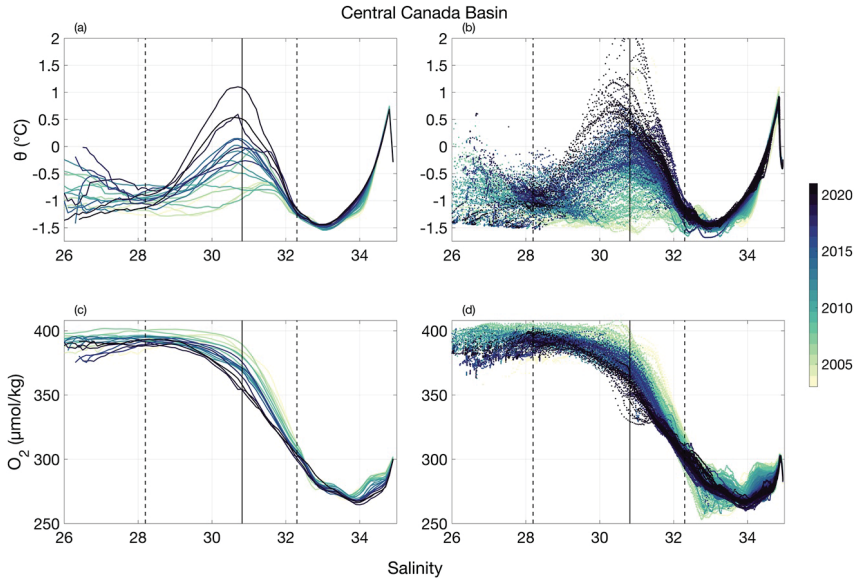

Figure 3. Potential temperature-salinity (θ-S) diagrams: (a) mean θ-S curves in each year (indicated by color) in the central Canada Basin (CB) and (b) all θ-S values (colored by year) in the central CB. O_2-S diagrams: (c) mean O_2-S curves in each year in the central CB region, and (d) all O_2-S values (colored by year) in the central CB. Dashed lines indicate mean salinities at Pacific Summer Water (PSW) bounds (see Section 2): depth of 30 m and $S = 32.3$, with a solid line indicating the mean salinity of the PSW temperature maximum.

in different portions of the PSW layer. To explore this further, it is useful to partition the PSW layer into upper and lower portions separated by the depth of the PSW temperature maximum. Although changes are in the same direction, the PSW tends to exhibit different trend magnitudes in its upper and lower portions suggesting different physical and biological mechanisms are at play. Changes expressed as linear trends (over 2003–2021) in upper and lower PSW layer-averaged properties are reported in Table 1. There are statistically significant increases in $\overline{\theta}$ (and decreases in $\overline{O_2}$ solubility) in both the upper and lower portions (Figure S4 in Supporting Information S1). In

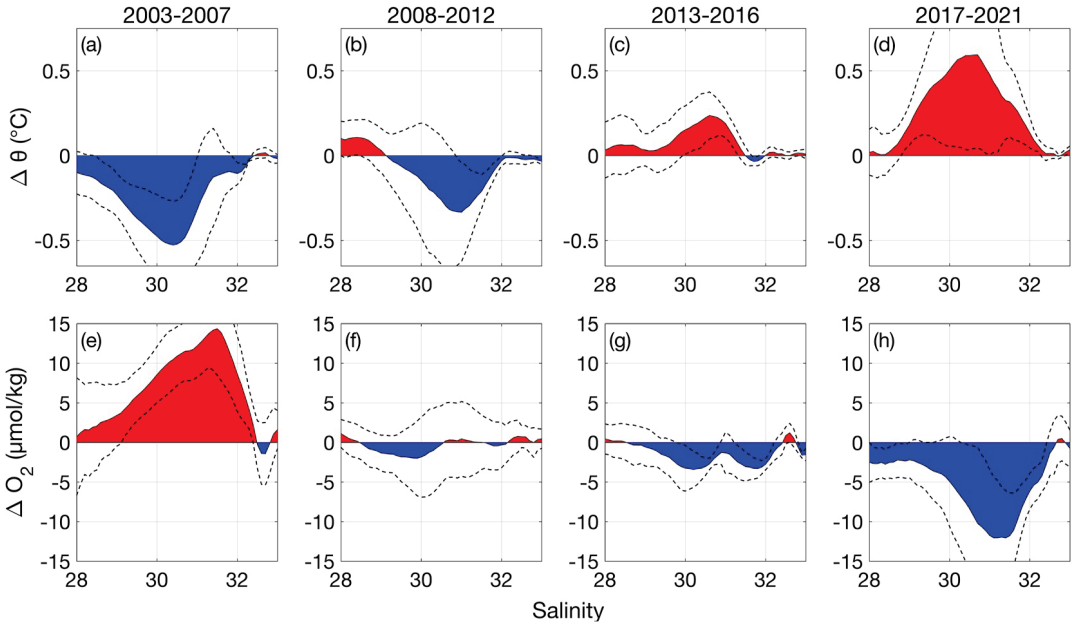

Figure 4. (a–d) Mean potential temperature (θ, °C) and (e–h) O_2 versus salinity anomalies of each year group (labeled at the top of each column) from the long term mean (2003–2021) in the central Canada Basin. The dashed lines indicate 1 standard deviation of the mean profiles in each year group.

Table 1
Linear Trends Over 2003–2021 (and 95% Confidence Intervals on the Linear Fit) for the Change in Layer-Averaged Upper and Lower Pacific Summer Water Portions in the CCB

Portion	$\overline{\theta}$ (°C yr^{-1})	$\overline{O_2}$ (μmol kg^{-1} yr^{-1})	$\overline{O_2}$ solubility (μmol kg^{-1} yr^{-1})	$\overline{AOU}$ (μmol kg^{-1} yr^{-1})
Upper PSW	+0.05 ± 0.01	−0.40 ± 0.15	−0.34 ± 0.07	+0.07 ± 0.13
Lower PSW	+0.03 ± 0.013	−0.61 ± 0.18	−0.27 ± 0.04	+0.34 ± 0.18

the upper portion, a statistically significant decrease in $\overline{O_2}$ can be entirely accounted for by the solubility change (i.e., there is no statistically significant change in $\overline{AOU}$). In the lower portion, the magnitude of the linear trend in $\overline{O_2}$ is about 0.21 μmol kg^{-1} yr^{-1} higher than in the upper portion, despite the $\overline{\theta}$ ($\overline{O_2}$ solubility) linear trend being about 0.02 °C yr^{-1} lower (Table 1, Figure S4 in Supporting Information S1). In lower PSW, the statistically significant trend in $\overline{AOU}$ suggests biological processes are likely contributing to the decreasing $\overline{O_2}$ trend observed in lower PSW.

5. Mechanisms for O_2 Change in PSW

Based on the trends described in the previous section, it is evident that different physical and biological processes are likely taking place in each of the upper and lower portions of the PSW. Next, we account for O_2 changes in the upper portion via an examination of the source waters for PSW in the CCB (i.e., where the CCB PSW was last in contact with the atmosphere). Then in Section 5.2 we present additional lines of evidence to explain the subtly different changes in the lower portion of the PSW.

5.1. Upper PSW

We hypothesize that O_2 decreases in CCB PSW over the period 2003–2021 are linked to PSW warming over the same period. Water masses with properties similar to PSW in the interior CB outcrop at the surface in the Chukchi Sea, which is consistent with CB halocline ventilation by Chukchi surface waters (Timmermans et al., 2017). Recent decades have seen reduced sea ice cover in the Northern Chukchi Sea and increased solar absorption there during summer; warming of these source waters for the CCB explains the warming trend in CCB PSW (Timmermans et al., 2018). As a consequence of their warming, Chukchi Sea surface waters have lower O_2 solubility, and likely reduced O_2 concentrations if equilibration with the atmosphere is the dominant control on O_2. To examine this, we analyze O_2 and temperature properties in the Chukchi Sea surface waters (Figure 5).

A surface front characterized by warm, saline, low O_2 waters in the Chukchi shelf region which transitions to cold, fresh, high O_2 near-surface waters in the CB region (north of the 300 m isobath; (see e.g., Timmermans et al., 2017)) is clearly visible in Figures 5a–5c. The strong agreement between temperature and O_2 values at 10 m depth in the Northern Chukchi Sea region (shown by the white box in Figure 5a) over the period 2000–2017 (Figure 5d) is consistent with the hypothesis that warmer near-surface potential temperatures in the northern Chukchi Sea are contributing to O_2 decreases in the CCB via the reduction in O_2 solubility. The O_2 decreases in upper PSW are entirely accounted for by the decreases in O_2 solubility (Table 1), and we infer that the main driver of O_2 decreases in this portion of PSW relates to the warming of Chukchi Sea surface waters, which then ventilate the CB.

5.2. Lower PSW

Statistically significant warming (decreasing $\overline{O_2}$ solubility) is observed in the lower PSW at a slower rate than for upper PSW (Table 1), while at the same time the rate of $\overline{O_2}$ decrease is faster than for upper PSW. Therefore, only a part of the $\overline{O_2}$ decrease in lower PSW can be accounted for by decreased $\overline{O_2}$ solubility that results from warming (as described in the previous section). The statistically significant trend in $\overline{AOU}$ increase in the lower PSW portion suggests that O_2 concentrations are likely also influenced by biological processes such as primary productivity or respiration/remineralization. Primary productivity may be elevated in recent years due to increased light availability as sea ice retreats (e.g., Ardyna & Arrigo, 2020; Arrigo & van Dijken, 2011, 2015; Stanley

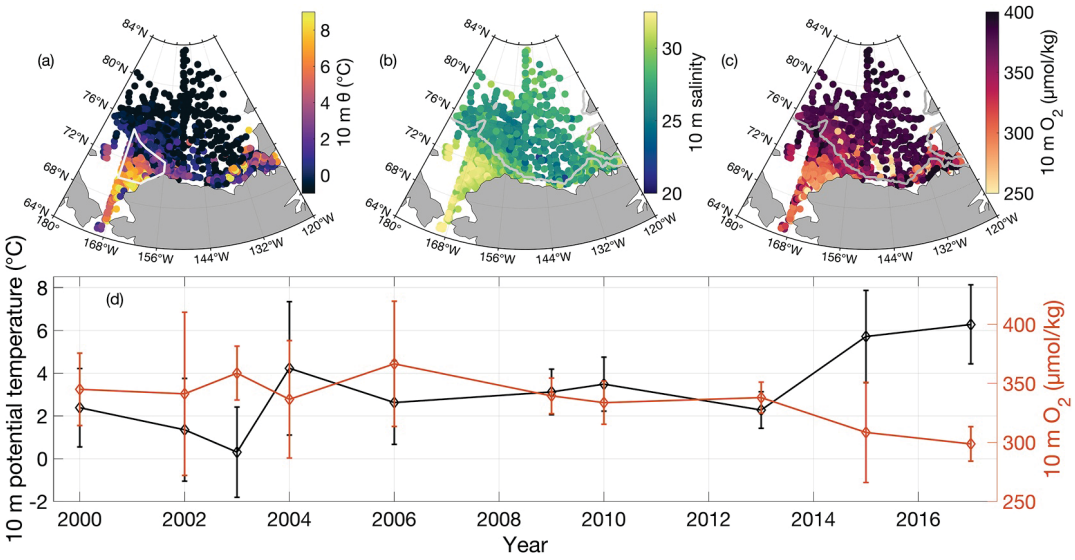

Figure 5. Maps of (a) potential temperature values at 10 m depth, where the white box indicates the Northern Chukchi Sea (defined as the region within 70°N to 73°N and 156°W to 170°W south of the 300 m isobath) (b) salinity values at 10 m depth and (c) O_2 values at 10 m depth (Data are from the World Ocean Database, including JOIS/BGOS data) (d) Time series of mean 10 m potential temperature (black) and 10 m O_2 (red) in the Northern Chukchi Sea (region defined in panel a) with error bars indicating 1 standard deviation over the region. Profiles were limited to July through September and span 2000–2017.

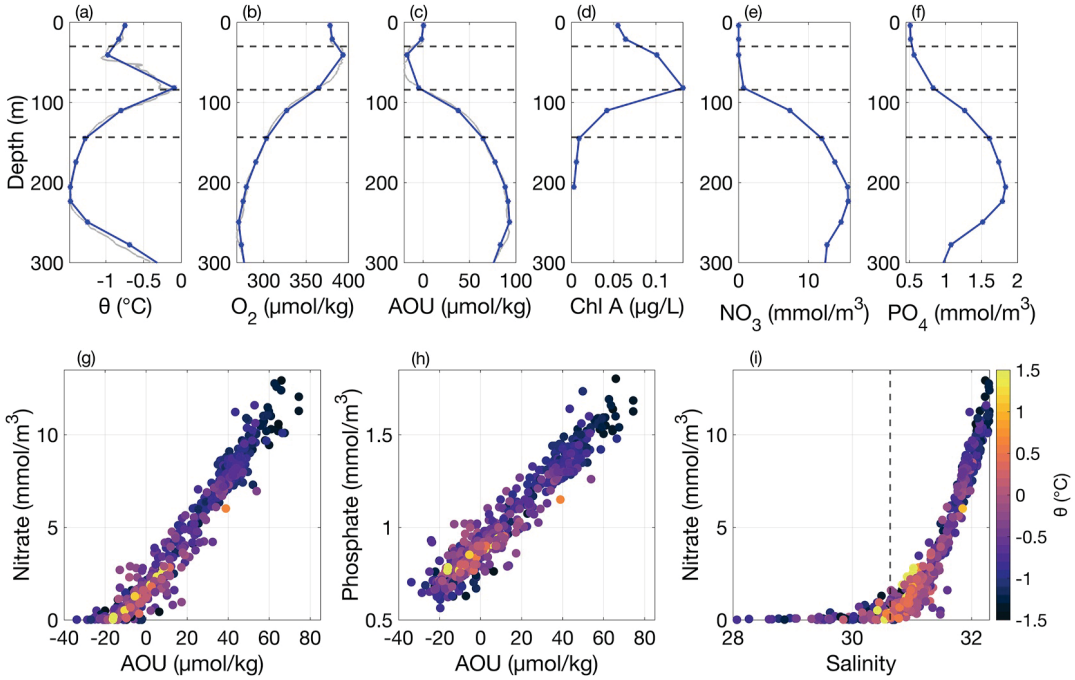

Figure 6. (a–f) Profiles from the 2017 JOIS/BGOS station located at 75.5°N 145°W (shown in Figure 1a) showing (a) potential temperature, (b) O_2, (c) Apparent Oxygen Utilization (AOU), (d) Chl A, (e) nitrate, and (f) phosphate versus depth. Data from the Niskin bottles are shown in blue, with the discrete depths marked as dots, while the continuous high resolution data are underlain in gray. The horizontal dashed lines in (a–f) denote depths of 30 m, the Pacific Summer Water (PSW) temperature maximum, and the $S = 32.3$ isohaline (bounds of upper and lower PSW). (g–i) Scatter plots of all PSW measurements (for all depths from 30 m to $S = 32.3$) across all years (2003–2021) showing (a) nitrate versus AOU (b) phosphate versus AOU and (c) nitrate versus salinity all colored by potential temperature. The vertical dashed line in (i) shows the average salinity at the PSW temperature maximum for all years.

et al., 2015). Although increased photosynthesis drives higher O_2 concentrations in the surface layer, a subsequent increased flux of organic matter raining down from the euphotic zone (and increased remineralization) can drive lower O_2 concentrations below the euphotic zone (Gilly et al., 2013). To examine this in context of lower PSW changes, we analyze nutrients (nitrate and phosphate) in these waters.

Nitrate and phosphate samples are from discrete depths (sampled by bottles on the Rosette) at lower vertical resolution compared to the higher vertical resolution O_2 and temperature profiles from the sensors (see e.g., Figures 6a and 6b). This results in issues when diagnosing trends in layer-averaged properties in the PSW. For example, the linear trends in layer-averaged O_2 and temperature inferred from the bottle data are inconsistent with the analogous trends in the CTD/SBE43 profiles in both upper and lower portions of the PSW. For this reason, we do not infer layer-averaged trends in nutrients. However, we can gain insight with the knowledge that AOU and nutrients are tightly coupled (Figures 6g and 6h); nutrients are consumed during primary production (AOU decreases) and regenerated during remineralization (AOU increases). Given the statistically significant increase in $\overline{\text{AOU}}$ in the lower PSW, and this tight coupling, it is reasonable to infer that there is likely increased organic matter breakdown/nutrient regeneration in the layer. Nutrient concentrations in the CCB are generally depleted at shallow depths, then increase with depth below the chlorophyll maximum (which coincides with the depth of the PSW temperature maximum, Figures 6a and 6d). This is consistent with the concept that a portion of the nutrients in the lower PSW are generated via organic matter remineralization (Figures 6c, 6e, and 6f), associated with the chlorophyll maximum. This is supported by the nitrate-salinity relationship with nitrate concentrations sharply increasing beneath the PSW temperature maximum (i.e., through the lower PSW, Figure 6i).

The question remains as to why there might be a trend toward increasing remineralization in the lower PSW. One expectation might be that the chlorophyll signal would suggest increased primary productivity and flux of organic matter into the lower PSW. However, the chlorophyll is seasonally varying, and given the different seasonal timing of the annual JOIS/BGOS expeditions, it is difficult to infer any trends. In the CB, nutrients are likely regenerated both locally and along the transit from the Chukchi Sea. Increased primary production observed in the Chukchi Sea (see e.g., Ardyna & Arrigo, 2020; Lewis et al., 2020) could be contributing to the increased signal of nutrient regeneration in lower PSW.

While we are not able to place bounds on primary productivity levels, we can evaluate the changes in O_2 consumption that may arise given the observed temperature increases. The rate at which O_2 is consumed during organic matter respiration, the apparent oxygen utilization rate (AOUR), follows an Arrhenius relationship which depends on water temperature (Alcaraz et al., 2013; Brewer & Peltzer, 2016; Brown et al., 2004). Ocean warming increases AOUR, such that sinking organic matter remineralizes more quickly and therefore at shallower depths (Breitburg et al., 2018). To investigate whether $\overline{\text{AOU}}$ increases in lower PSW may be accounted for by increased respiration rates due to PSW warming, we estimate changes in AOUR as $\text{AOUR} = \text{A}e^{-\frac{\text{Ea}}{\text{R}\overline{\theta}}}$ (see Brewer & Peltzer, 2017), where A is a constant (the exact value does not matter, as we are interested in quantifying percent changes in AOUR, not their absolute values), Ea is the activation energy (kJ mol^{-1}), R is the ideal gas constant (8.314 J K^{-1} mol^{-1}), and $\overline{\theta}$ is the lower PSW layer-averaged potential temperature (K). Activation energies for Arctic Ocean respiration have been reported to range between about 14 and 220 kJ mol^{-1} (see Vaquer-Sunyer et al., 2010). Considering this full range, and the observed warming of the lower PSW, AOUR could be expected to have increased by about ~2%–22%, which would lead to $\overline{\text{AOU}}$ increases of +0.03–0.30 μmol kg^{-1} yr^{-1} over 2003–2021. This is of comparable magnitude to the linear $\overline{\text{AOU}}$ trend in lower PSW over the same time frame (+0.34 ± 0.18 μmol kg^{-1}). Therefore, in the lower portion of PSW, both the effects of decreased $\overline{O_2}$ solubility and increased respiration rates as a result of lower PSW warming, would seem to account for the observed $\overline{O_2}$ decrease in approximately equal measure. We note, however, that changes in surface equilibrium in the Chukchi Sea (i.e., oversaturation or undersaturation with changes in primary productivity or ice cover, for example) could influence this interpretation. In addition, changes in boundary currents in the Chukchi shelf region could influence surface O_2 via changes in air-sea fluxes and transport of organic material/nutrients (e.g., Danielson et al., 2017). Additional nutrient data, including in the source region for PSW, are needed to better understand nutrient origins and evolution and links to AOU in the CCB PSW.

6. Summary and Discussion

Sustained annual sampling over 2003–2021 of dissolved oxygen in PSW in the CB halocline shows O_2 decreasing in this water mass commensurate with increasing temperatures. Overall, the PSW layer-averaged O_2 has decreased

by about 5% (from values around 355 μmol kg^{-1} in 2003 to 340 μmol kg^{-1} in 2021) while layer-averaged potential temperature has increased from values around −0.86°C in 2003 to −0.36°C in 2021. Rates of decrease of $\overline{O_2}$ differ between the upper and lower portions of the PSW, with larger $\overline{O_2}$ reduction in the lower portion. Related trends in Chukchi Sea surface waters (source waters for the CB PSW halocline), along with the lack of a significant trend in upper PSW $\overline{AOU}$ indicate that decreased $\overline{O_2}$ solubility can entirely account for reduced $\overline{O_2}$ in the upper portion of the PSW, which resides above the chlorophyll maximum. Despite there being no significant change in upper PSW $\overline{AOU}$ over the study period, upper PSW warming could be leading to increased organic matter respiration rates in the layer. Since AOU accounts for both primary productivity and respiration, the effect of accelerated respiration rates in upper PSW (which consume O_2) could potentially be counteracted by increased primary production in the layer (which produces O_2) due to the effects of sea-ice decline (e.g., Ardyna & Arrigo, 2020; Arrigo & van Dijken, 2011, 2015). In the lower portion of PSW, decreased solubility also contributes to declining $\overline{O_2}$, with an additional factor related to the breakdown of sinking organic matter (the lower PSW resides below the chlorophyll maximum). A statistically significant positive trend in $\overline{AOU}$ in lower PSW (along with the tight relationship between AOU and nutrients) points to increased organic matter remineralization in the lower PSW. The required increased respiration rates are consistent with expectations in warming waters. Increased primary production in upper PSW and source waters would also likely lead to an increased flux of organic matter into the lower PSW portion, potentially contributing to the observed increase in organic matter breakdown in lower PSW.

In recent decades, decreases in O_2 have been observed globally owing to physical factors (e.g., changes in solubility and ventilation rates) and biogeochemical factors (e.g., changes in primary production/respiration and nutrient availability) (e.g., Breitburg et al., 2018; Keeling et al., 2010; Robinson, 2019). The rates of decreasing oxygen concentrations in both upper and lower PSW over 2003–2021 (Table 1) exceed global upper ocean (0–1,000 m) averages of oxygen decline over 1970–2010 (−0.08 μmol kg^{-1} yr^{-1}) as reported in the 2021 IPCC Sixth Assessment Report (Gulev et al., 2021) by an order of magnitude. Other regions where declines in upper ocean oxygen concentrations over various time scales exceed the global upper ocean rates include areas of the North Pacific, the Southern Ocean, and the Indian Ocean (see Gulev et al., 2021). Elsewhere in the global ocean where conditions can approach hypoxic (i.e., having O_2 concentrations <60 μmol kg^{-1}, e.g., Tremblay et al. (2020)), decreasing O_2 concentrations are leading to widespread reductions in biodiversity and habitat availability (Breitburg et al., 2018). While the CB water column is far from hypoxic, substantial warming and a continued trajectory to lower water-column O_2 highlights the need for continued monitoring of physical and biogeochemical properties, and studies to understand the implications to polar ecosystems of the changes underway.

Data Availability Statement

Data are from the Beaufort Gyre Exploration Program, and are available here: https://www2.whoi.edu/site/beaufortgyre/. Additional hydrographic data are from the World Ocean Database 2018, and are available here: https://www.ncei.noaa.gov/products/world-ocean-database.

Acknowledgments
The data were collected and made available by the Beaufort Gyre Exploration Program based at the Woods Hole Oceanographic Institution (https://www2.whoi.edu/site/beaufortgyre/) in collaboration with researchers from Fisheries and Oceans Canada at the Institute of Ocean Sciences. Funding for this study was provided by the National Science Foundation Division of Polar Programs under Grant 1950077. Special thanks to Andrey Proshutinsky for helpful input.

References

Aagaard, K., Coachman, L., & Carmack, E. (1981). On the halocline of the Arctic Ocean. *Deep-Sea Research, Part A: Oceanographic Research Papers*, *28*(6), 529–545. https://doi.org/10.1016/0198-0149(81)90115-1

Alcaraz, M., Almeda, R., Saiz, E., Calbet, A., Duarte, C. M., Agustí, S., et al. (2013). Effects of temperature on the metabolic stoichiometry of Arctic zooplankton. *Biogeosciences*, *10*(2), 689–697. https://doi.org/10.5194/bg-10-689-2013

Ardyna, M., & Arrigo, K. R. (2020). Phytoplankton dynamics in a changing Arctic Ocean. *Nature Climate Change*, *10*(10), 892–903. https://doi.org/10.1038/s41558-020-0905-y

Ardyna, M., Babin, M., Gosselin, M., Devred, E., Bélanger, S., Matsuoka, A., & Tremblay, J.-É. (2013). Parameterization of vertical chlorophyll a in the Arctic Ocean: Impact of the subsurface chlorophyll maximum on regional, seasonal, and annual primary production estimates. *Biogeosciences*, *10*(6), 4383–4404. https://doi.org/10.5194/bg-10-4383-2013

Arrigo, K. R., & van Dijken, G. L. (2011). Secular trends in Arctic Ocean net primary production. *Journal of Geophysical Research*, *116*(C9), C09011. https://doi.org/10.1029/2011jc007151

Arrigo, K. R., & van Dijken, G. L. (2015). Continued increases in Arctic Ocean primary production. *Progress in Oceanography*, *136*, 60–70. https://doi.org/10.1016/j.pocean.2015.05.002

Barwell-Clarke, J., & Whitney, F. (1996). *Institute of Ocean Sciences nutrient methods and analysis*. Citeseer.

Boyer, T., Baranova, O., Coleman, C., Garcia, H., Grodsky, A., Locarnini, R., et al. (2018). *World Ocean Database 2018* (Vol. 87). NOAA Atlas NESDIS.

Breitburg, D., Levin, L. A., Oschlies, A., Grégoire, M., Chavez, F. P., Conley, D. J., et al. (2018). Declining oxygen in the global ocean and coastal waters. *Science*, *359*(6371), eaam7240. https://doi.org/10.1126/science.aam7240

Brewer, P. G., & Peltzer, E. T. (2016). Ocean chemistry, ocean warming, and emerging hypoxia: Commentary. *Journal of Geophysical Research: Oceans*, *121*(5), 3659–3667. https://doi.org/10.1002/2016jc011651

Brewer, P. G., & Peltzer, E. T. (2017). Depth perception: The need to report ocean biogeochemical rates as functions of temperature, not depth. *Philosophical Transactions of the Royal Society A: Mathematical, Physical & Engineering Sciences*, *375*(2102), 20160319. https://doi.org/10.1098/rsta.2016.0319

Brown, J. H., Gillooly, J. F., Allen, A. P., Savage, V. M., & West, G. B. (2004). Toward a metabolic theory of ecology. *Ecology*, *85*(7), 1771–1789. https://doi.org/10.1890/03-9000

Coachman, L., & Barnes, C. (1961). The contribution of Bering Sea water to the Arctic Ocean. *Arctic*, *14*(3), 147–161. https://doi.org/10.14430/arctic3670

Danielson, S. L., Eisner, L., Ladd, C., Mordy, C., Sousa, L., & Weingartner, T. J. (2017). A comparison between late summer 2012 and 2013 water masses, macronutrients, and phytoplankton standing crops in the northern Bering and Chukchi Seas. *Deep Sea Research Part II: Topical Studies in Oceanography*, *135*, 7–26. https://doi.org/10.1016/j.dsr2.2016.05.024

Eveleth, R., Timmermans, M.-L., & Cassar, N. (2014). Physical and biological controls on oxygen saturation variability in the upper Arctic Ocean. *Journal of Geophysical Research: Oceans*, *119*(11), 7420–7432. https://doi.org/10.1002/2014jc009816

Falkner, K. K., Steele, M., Woodgate, R. A., Swift, J. H., Aagaard, K., & Morison, J. (2005). Dissolved oxygen extrema in the Arctic Ocean halocline from the North Pole to the Lincoln sea. *Deep Sea Research Part I: Oceanographic Research Papers*, *52*(7), 1138–1154. https://doi.org/10.1016/j.dsr.2005.01.007

Garcia, H. E., Boyer, T. P., Locarnini, R. A., Antonov, J. I., Mishonov, A. V., Baranova, O. K., et al. (2013). World Ocean Atlas 2013. Volume 3, dissolved oxygen, apparent oxygen utilization, and oxygen saturation.

Garcia, H. E., & Gordon, L. I. (1992). Oxygen solubility in seawater: Better fitting equations. *Limnology & Oceanography*, *37*(6), 1307–1312. https://doi.org/10.4319/lo.1992.37.6.1307

Gilly, W. F., Beman, J. M., Litvin, S. Y., & Robison, B. H. (2013). Oceanographic and biological effects of shoaling of the oxygen minimum zone. *Annual Review of Marine Science*, *5*(1), 393–420. https://doi.org/10.1146/annurev-marine-120710-100849

Gulev, S., Thorne, P., Ahn, J., Dentener, F., Domingues, C., Gerland, S., et al. (2021). *Climate change 2021: The physical science basis. Contribution of working group I to the sixth assessment report of the intergovernmental panel on climate change [book section]*. In V. Masson-Delmotte, P. Zhai, A. Pirani, S. L. Connors, C. Péan, S. Berger, et al. (Eds.), (pp. 287–422). Cambridge University Press.

Keeling, R. F., Körtzinger, A., & Gruber, N. (2010). Ocean deoxygenation in a warming world. *Annual Review of Marine Science*, *2*(1), 199–229. https://doi.org/10.1146/annurev.marine.010908.163855

Koeve, W., & Kähler, P. (2016). Oxygen utilization rate (OUR) underestimates Ocean respiration: A model study. *Global Biogeochemical Cycles*, *30*(8), 1166–1182. https://doi.org/10.1002/2015gb005354

Lewis, K., Van Dijken, G., & Arrigo, K. R. (2020). Changes in phytoplankton concentration now drive increased Arctic Ocean primary production. *Science*, *369*(6500), 198–202. https://doi.org/10.1126/science.aay8380

Martin, J., Tremblay, J., & Price, N. (2012). Nutritive and photosynthetic ecology of subsurface chlorophyll maxima in Canadian Arctic waters. *Biogeosciences*, *9*(12), 5353–5371. https://doi.org/10.5194/bg-9-5353-2012

McLaughlin, F., Carmack, E., O'Brien, M., Barwell-Clarke, J., Gatien, G., Harris, J., et al. (2009). Physical and chemical data from the Beaufort Sea and Canada basin, August 16 to September 5, 2002. *Canadian Data Report of Hydrography and Ocean Sciences*, *181*.

Ouyang, Z., Qi, D., Zhong, W., Chen, L., Gao, Z., Lin, H., et al. (2021). Summertime evolution of net community production and CO_2 flux in the western Arctic Ocean. *Global Biogeochemical Cycles*, *35*(3), e2020GB006651. https://doi.org/10.1029/2020gb006651

Robinson, C. (2019). Microbial respiration, the engine of ocean deoxygenation. *Frontiers in Marine Science*, *5*, 533. https://doi.org/10.3389/fmars.2018.00533

Stanley, R. H., Sandwith, Z. O., & Williams, W. J. (2015). Rates of summertime biological productivity in the Beaufort Gyre: A comparison between the low and record-low ice conditions of August 2011 and 2012. *Journal of Marine Systems*, *147*, 29–44. https://doi.org/10.1016/j.jmarsys.2014.04.006

Steele, M., Morison, J., Ermold, W., Rigor, I., Ortmeyer, M., & Shimada, K. (2004). Circulation of summer Pacific halocline water in the Arctic Ocean. *Journal of Geophysical Research*, *109*(C2), C02027. https://doi.org/10.1029/2003jc002009

Timmermans, M.-L., Krishfield, R., Laney, S., & Toole, J. (2010). Ice-tethered profiler measurements of dissolved oxygen under permanent ice cover in the Arctic Ocean. *Journal of Atmospheric and Oceanic Technology*, *27*(11), 1936–1949. https://doi.org/10.1175/2010jtecho772.1

Timmermans, M.-L., Marshall, J., Proshutinsky, A., & Scott, J. (2017). Seasonally derived components of the Canada Basin halocline. *Geophysical Research Letters*, *44*(10), 5008–5015. https://doi.org/10.1002/2017gl073042

Timmermans, M.-L., Proshutinsky, A., Golubeva, E., Jackson, J., Krishfield, R., McCall, M., et al. (2014). Mechanisms of Pacific summer water variability in the Arctic's Central Canada Basin. *Journal of Geophysical Research: Oceans*, *119*(11), 7523–7548. https://doi.org/10.1002/2014jc010273

Timmermans, M.-L., Toole, J., & Krishfield, R. (2018). Warming of the interior Arctic Ocean linked to sea ice losses at the basin margins. *Science Advances*, *4*(8), eaat6773. https://doi.org/10.1126/sciadv.aat6773

Timmermans, M.-L., & Toole, J. M. (2023). The Arctic Ocean's Beaufort Gyre. *Annual Review of Marine Science*, *15*(1), 223–248. https://doi.org/10.1146/annurev-marine-032122-012034

Tremblay, N., Hünerlage, K., & Werner, T. (2020). Hypoxia tolerance of 10 Euphausiid species in relation to vertical temperature and oxygen gradients. *Frontiers in Physiology*, *11*, 248. https://doi.org/10.3389/fphys.2020.00248

Vaquer-Sunyer, R., Duarte, C. M., Santiago, R., Wassmann, P., & Reigstad, M. (2010). Experimental evaluation of planktonic respiration response to warming in the European Arctic Sector. *Polar Biology*, *33*(12), 1661–1671. https://doi.org/10.1007/s00300-010-0788-x

Weingartner, T. J., Danielson, S. L., & Royer, T. C. (2005). Freshwater variability and predictability in the Alaska coastal current. *Deep Sea Research Part II: Topical Studies in Oceanography*, *52*(1–2), 169–191. https://doi.org/10.1016/j.dsr2.2004.09.030

Woodgate, R. A., Aagaard, K., & Weingartner, T. J. (2005). A year in the physical oceanography of the Chukchi Sea: Moored measurements from autumn 1990–1991. *Deep Sea Research Part II: Topical Studies in Oceanography*, *52*(24–26), 3116–3149. https://doi.org/10.1016/j.dsr2.2005.10.016

Zhong, W., Steele, M., Zhang, J., & Cole, S. T. (2019). Circulation of Pacific winter water in the Western Arctic Ocean. *Journal of Geophysical Research: Oceans*, *124*(2), 863–881. https://doi.org/10.1029/2018jc014604